QUANTUM SOLIDS

10.1126/sciadv.1500825

Equilibrium shape of ^{4}He crystal under zero gravity below 200 mK

Takuya Takahashi, Haruka Ohuchi, Ryuji Nomura,* Yuichi Okuda

Equilibrium crystal shape is the lowest energy crystal shape that is hardly realized in ordinary crystals because of their slow relaxation. ^{4}He quantum crystals in a superfluid have been expected as unique exceptions that grow extremely fast at very low temperatures. However, on the ground, gravity considerably deforms the crystals and conceals the equilibrium crystal shape, and thus, gravity-free environment is needed to observe the equilibrium shape of ^{4}He. We report the relaxation processes of macroscopic ^{4}He crystals in a superfluid below 200 mK under zero gravity using a parabolic flight of a jet plane. When gravity was removed from a gravity-flattened ^{4}He crystal, the crystal rapidly transformed into a shape with flat surfaces. Although the relaxation processes were highly dependent on the initial condition, the crystals relaxed to a nearly homothetic shape in the end, indicating that they were truly in an equilibrium shape minimizing the interfacial free energy. Thanks to the equilibrium shape, we were able to determine the Wulff's origin and the size of the c-facet together with the vicinal surface profile next to the c-facet. The c-facet size was extremely small in the quantum crystals, and the facet-like flat surfaces were found to be the vicinal surfaces. At the same time, the interfacial free energy of the a-facet and s-facet was also obtained.

INTRODUCTION

The equilibrium crystal shape (ECS) reflects a large amount of physical information, such as the angular dependence of the interfacial free energy, the existence of a roughening transition, and the dependence of step-step interaction on the step interval (*1*). Thus, the observation of the ECS is one of the most direct and convincing methods to investigate crystalline properties. However, practical realization of the ECS is very difficult because of the very poor interface motion of crystals, which hinders the equilibration process. All macroscopic crystals observed are those that are quenched during growth. One unique exception is the ^{4}He quantum crystal grown from a superfluid at low temperatures. In the ^{4}He crystal–superfluid system at low temperatures, the crystal growth coefficient is determined by the scattering of elementary excitations within the system. As the temperature decreases toward $T = 0$ K, the growth coefficient becomes divergently large enough for the ^{4}He crystal to reach an equilibrium state in an extremely short period (*2*). Thus, the ^{4}He crystal is the most probable candidate for the observation of ECS. Down to 300 mK, three types of facets, (0001), $(10\bar{1}0)$, and $(10\bar{1}1)$, are known to exist in hexagonal close-packed ^{4}He crystals and are referred to as c-facet, a-facet, and s-facet, respectively (*2*).

However, as a further problem concerning ECS experiments on the ground, the effect of gravity must be excluded because gravity considerably deforms the crystal and conceals the ECS that is purely determined by the interfacial free energy. The interfacial free energy should dominate the formation of the crystal, as long as the crystal is much smaller than the capillary length $l_c = (\alpha/\Delta\rho g)^{1/2}$, where α, $\Delta\rho$, and g are the interfacial free energy, the density difference between the two phases, and the gravity acceleration, respectively. The capillary length of a ^{4}He crystal under the gravity on the ground is about 1 mm, and measurement on the limited scale would be difficult and produce ambiguities. Furthermore, the ^{4}He crystal is a typical quantum crystal, where the magnitude of the fluctuations of atoms around their lattice sites is large. As a consequence, the liquid-solid interface is anomalously thick so that the lattice influence on the interface position is weak. This is a case of so-called weak coupling. One consequence of this weak coupling is that the step energy β is small compared to $a\alpha$, where a is the period of the lattice in the direction perpendicular to the facet. The ratio of $\beta/a\alpha_c$ is proportional to the ratio of the facet size to the crystal size; in the case of ^{4}He, the size of the c-facet is estimated to be as small as $^1/_{10}$ of the total crystal size (*2*). Thus, to resolve such fine structure of the true ECS, a macroscopic crystal that is free from deformation by gravity is required. Therefore, a zero-gravity environment is necessary for research on the ECS with ^{4}He crystals. There are several theoretical studies on the effect of gravity on the ECS that can support experimentation with ^{4}He crystals (*3*–*5*). Here, we report the first very low temperature experiment under zero gravity to investigate the ECS of ^{4}He crystals using a customized ^{3}He-^{4}He dilution refrigerator. The parabolic flight of a small jet plane was adopted to produce a low-gravity environment of less than $0.01g$, which can be regarded as practically zero gravity for the present experiment.

RESULTS

^{4}He crystal with a nonhorizontal c-facet

The first example of ^{4}He crystal shape transformation is shown in Fig. 1 at about 150 mK under zero gravity. A video clip of this process is provided in movie S1. Initially, a rough horizontal surface was dominant under gravity to minimize the gravitational energy, and a small c-facet appeared near the right-side wall (Fig. 1A). As soon as reduction of the gravity began (Fig. 1B), the rough surface upheaved to retrieve the deformation by gravity, which resulted in expansion of the c-facet (Fig. 1, C to F) and the appearance of an a-facet on the left side of the crystal (Fig. 1F). Similar behavior was observed for the c-facet and a-facet at a much higher temperature of 600 mK under zero gravity using a ^{3}He evaporation refrigerator (*6*). Compared to the high-temperature experiment in which the s-facet was absent, the interface at 150 mK was more responsive to vibrations of the system because of the higher mobility of the crystal surface at lower temperature. The vibrations were caused by air turbulence at the altitude where the parabolic flight was performed.

Department of Physics, Tokyo Institute of Technology, 2-12-1 Ookayama, Meguro, Tokyo 152-8551, Japan.
*Corresponding author. E-mail: nomura.r.aa@m.titech.ac.jp

The s-facet emerged between the c-facet and a-facet (Fig. 1, F to J), although it was often blurred by the frequent vibrations caused by the turbulence. The s-facet was reported to have an angle of 58.5° to the c-facet (*2*), which was consistent with our observation. This was the first direct recognition of an s-facet for an equilibrium state that was essential for later analysis, although the s-facet was previously observed on a slowly growing ^{4}He crystal below 365 mK (*7*). When gravity had returned after the parabolic flight, the crystal quickly returned to the initial shape (Fig. 1, K and L) as the reverse process. The crystal did not spontaneously detach from the wall during parabolic flight because of partial wetting of the crystal.

^{4}He crystal with a nearly horizontal c-facet

The crystalline orientation with respect to the wall had a strong influence on the transformation process after the reduction of gravity. As a second example, a crystal was prepared with the c-facet almost horizontally, and no rough surface appeared except for a small region near the contact point with the wall. No significant interface motion of the crystal was observed in this case, as shown in Fig. 2 (A to C). The only noticeable change was that the curvature of the rough surface near the contact point became smaller under reduced gravity, which reflects an enlargement of the capillary length (Fig. 2, B and C). As a result of the curvature variation, the c-facet grew slightly in the vertical direction, although this small amount of facet motion is difficult to recognize with the scale of these figures. The crystal transformation immediately ceased after the reduction of gravity, and the shape remained until the gravity was recovered, unless the crystal was perturbed to a large extent. Pinning by the wall was so strong that the crystal was not able to escape from this metastable condition set by the wall. The cessation of the crystal transformation was not attributed to the small growth coefficient of the facet but to the completion of relaxation to the equilibrium state under this pinned condition.

An attempt was made to deform the crystal in Fig. 2 during the zero-gravity period with an acoustic wave pulse, which can be used to manipulate the crystal on the ground (*8*–*10*). An acoustic wave pulse was applied for 0.5 s from the lower part of the cell to hit the interface in the upward direction. The central region of the interface (c-facet) where the acoustic wave impacted was cylindrically deformed, moved upward via crystallization induced by the acoustic radiation pressure, and reached the ceiling (Fig. 2, D to F). On the top of the growing interface,

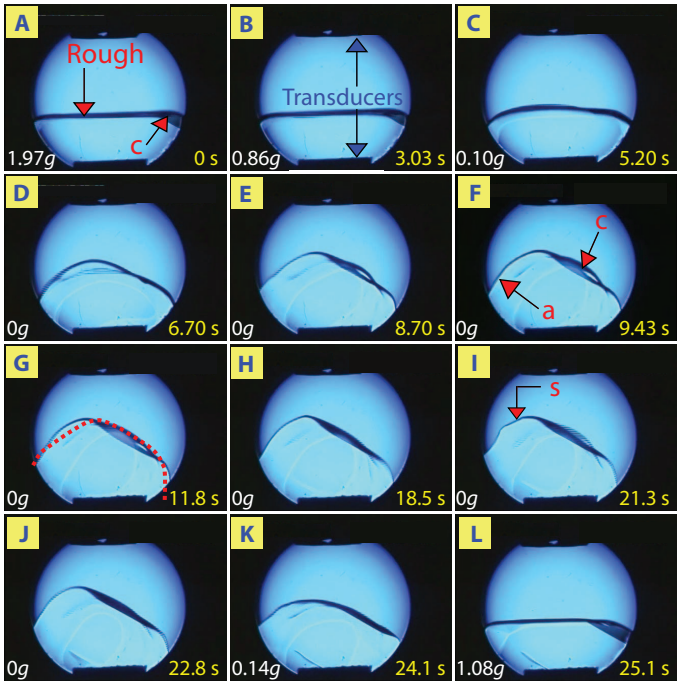

Fig. 1. Transformation of a ^{4}He crystal with nonhorizontal c-facet via a sudden reduction of gravity. (**A** to **L**) Gravity values and times elapsed are presented in each frame. The orientation of the c-facet was inclined from the horizontal plane. Under gravity, a rough horizontal surface covered most part of the crystal, and a c-facet appeared in a small portion of the crystal in the vicinity of the wall, as indicated by the arrows in (A). Under zero-gravity conditions, the crystal transformed into a different stable shape, and c-facet, a-facet, and s-facet became visible.

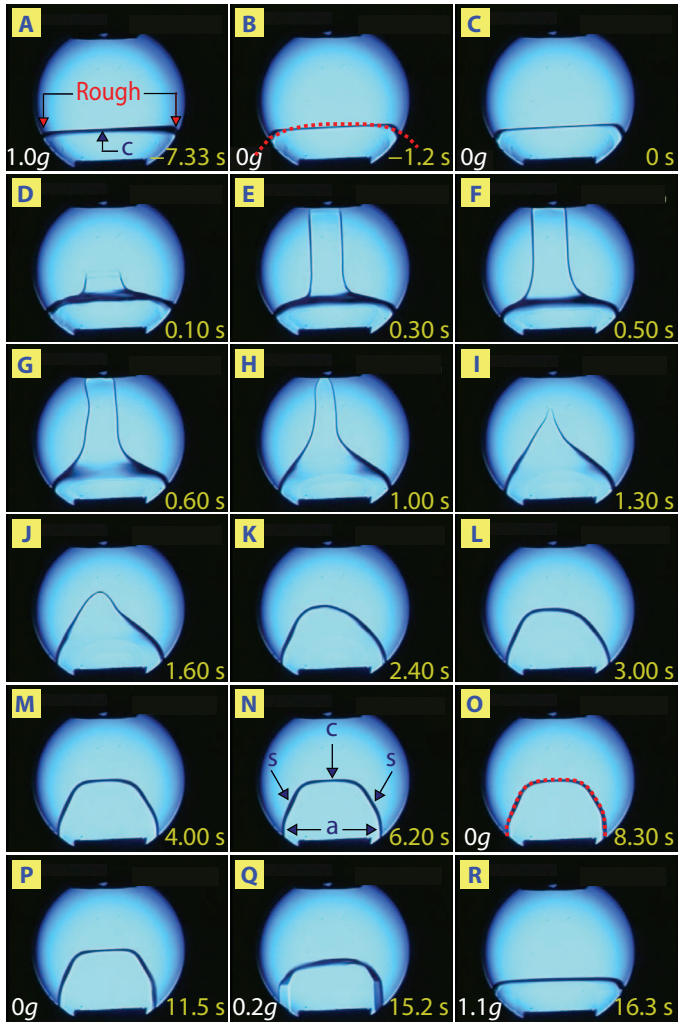

Fig. 2. Transformation of a ^{4}He crystal with nearly horizontal c-facet via a sudden reduction of gravity. (**A** to **R**) The reduction of gravity did not significantly affect the crystal shape (A to C). The successive pictures (D to P) show the deformation process of the ^{4}He crystal by an acoustic wave pulse and the subsequent relaxation process after the pulse was turned off. The deformed crystal relaxed to an equilibrium shape different from the initial shape. After the zero-gravity period (Q and R), the crystal recovered the initial shape as in (A).

a c-facet was clearly observed and provides evidence that the deformation was due to crystallization. After the acoustic wave pulse was turned off, the top of the cylinder detached from the ceiling, became rounded (Fig. 2H), and then changed into a cone-like shape (Fig. 2I) that was absorbed into the main body of the crystal, whereas the upper surface of the body grew slightly (Fig. 2, J to L). The crystal shape in Fig. 2K was rounded and the c-facet completely disappeared from the interface because of the large perturbation. Subsequently, the c-facet, a-facet, and s-facet spontaneously appeared from the rough surface (Fig. 2M), and the images shown in Fig. 2 (M to P) are considered to be the ECS. The deformation unpinned the contact line between the wall, liquid, and crystal and allowed the crystal to escape from the metastable condition; the relaxation processes accompanied the recession of the contact line. Thus, the deformed crystal relaxed to a completely different shape from the previous shapes shown in Fig. 2 (B and C).

After the zero-gravity period (Fig. 2, Q and R), the crystal recovered the initial shape as in Fig. 2A. This indicates that neither unwanted rotation of the crystal nor regrowth of a crystal of different orientation was induced by the acoustic wave pulse during the zero gravity; the crystal maintained the original orientation during the zero gravity. A video clip of Fig. 2 is provided in movie S2.

After the acoustic wave pulse temporarily increased the temperature of the cell above 330 mK, it was cooled down to about 220 mK within a few seconds. Figure 3 shows the time evolution of the temperature for the sample cell and the mixing chamber together with the gravity. Considering the flatness of the ^{4}He crystal melting curve, the small variation of the temperature at about 200 mK would not have any influence on the crystal shape.

DISCUSSION

The relaxed shape in Fig. 2 (M to P) is similar to those in Fig. 1 (F to J) and Fig. 2 (B and C), despite the different onsets of the relaxation processes due to the different initial conditions. The red dotted curves in Figs. 1G and 2 (B and O) are homothetic, which accounts for the hypothesis that each crystal reached the equilibrium state.

A two-dimensional equilibrium crystal profile of a c-facet and the adjacent vicinal surface was theoretically predicted (*11*, *12*) as Eq. 1, with the assumption of a step-step interaction energy of the form σ/r^2 (*1*, *13*, *14*)

$$z(x) = -\frac{2}{3}\sqrt{\frac{a^3\Delta\mu}{3\sigma v_s}}(x - R_F)^{3/2} \quad (1)$$

where z represents the height variation from the facet ($z = 0$), x ($x \geq R_F$) denotes the distance from the center of the facet, $\Delta\mu$ is the chemical potential difference between the crystal and the ambient phase, σ is the step-step interaction coefficient, and r is the step interval. The radius of the c-facet R_F is expressed as $\beta v_s/a\Delta\mu$, where v_s is the crystal volume per unit atom. In addition, as long as the crystal is in the equilibrium state, the following relation holds for any i-th plane of the crystal

$$\frac{\alpha_i}{h_i} = \frac{\Delta\mu}{2v_s} \quad (2)$$

which is known as the Wulff theorem (*15*). Here, α_i is the interfacial free energy of i-th plane, and h_i is the distance between the i-th plane and the origin of the polar plot in the Wulff construction (Wulff's origin) of the ECS.

R_F is derived from Eq. 2 as $\beta h_c/2a\alpha_c$, where the indices represent the values of the c-facet, and is proportional to the characteristic crystal length and the ratio $\beta/a\alpha_c$. As with the c-facet of the ^{4}He crystal, the ratio is about $^1/_{10}$; thus, R_F should be much smaller than the crystal size (*2*). However, despite this small ratio, a much larger flat region that is approximately half of the crystal size and parallel to the c-facet is apparent in Figs. 1 and 2.

To solve this discrepancy in the appearance, we compared the observed crystal profile with the numerical curve $z(x)$ calculated using Eq. 1. For that purpose, the value of $\Delta\mu/v_s$ was needed and could be obtained from Eq. 2 using the distance between the origin and the c-facet, h_c. The origin of the Wulff plot was determined on the basis of the simple assumption that the perpendicular bisectors of the c-facet and s-facet pass through the origin, neglecting a small orientation dependency of the interfacial free energy around the s-facet. Because the s-facet appeared clearly at the experimental temperature, the position of the origin could be successfully specified with reasonably good accuracy and is indicated by the open circle in Fig. 4A for the final relaxed crystal in Fig. 2. The dashed lines in Fig. 4A are the perpendicular bisectors of each facet. After the origin is determined, the distances between the origin and each

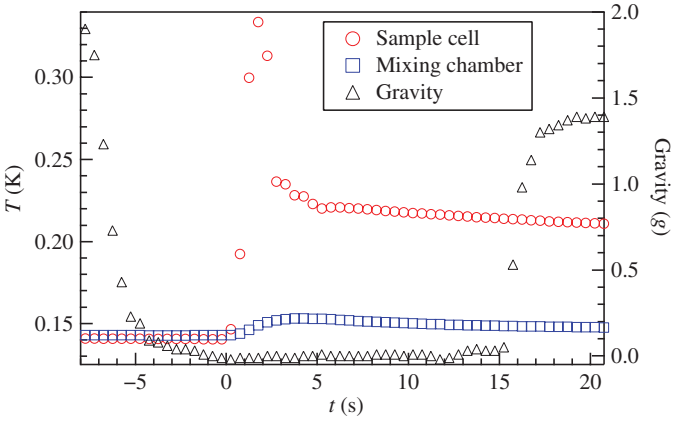

Fig. 3. Time evolution of the temperature and gravity. Temperature of the sample cell and the mixing chamber due to the application of acoustic wave pulse was recorded with the gravity.

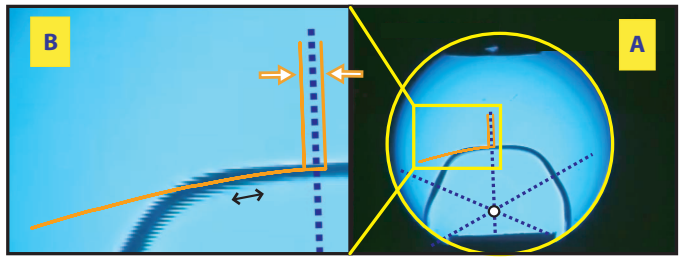

Fig. 4. Comparison of the facet-like flat surface parallel to the c-facet of the final relaxed crystal in Fig. 2 with the theoretical curve obtained using Eq. 1. (**A** and **B**) This comparison suggests that the true facet appears on the narrow area between the open arrows and the vicinal surface occupies the other area. Around the two-headed arrows, the curve deviates from the surface, where the surface transforms from the vicinal state to the rough state. The open circle located at the intersection point between the perpendicular bisectors (the dashed lines) of the c-facet and s-facet indicates the origin in the Wulff construction.

Table 1. Distances from the Wulff's origin of the crystal to each facet and the interfacial free energy derived from the distances. Crystal 1 (*2*) corresponds to the relaxed crystal in Fig. 1 (*2*). The indices represent each facet (c, a, and s). Errors are derived from the ambiguity in the determination of the Wulff's origin.

	h_c (mm)	h_a	h_s	α_a (erg/cm^2)	α_s
Crystal 1	9.1	10.3	10.6	0.195 ± 0.011	0.200 ± 0.009
Crystal 2	7.0	7.8	7.5	0.192 ± 0.015	0.184 ± 0.009

facet can be measured from the pictures, and the interfacial free energy of the a-facet and s-facet, α_a and α_s, can be simultaneously extracted from Eq. 2 by adopting that for the c-facet of the ^{4}He crystal as $\alpha_c = 0.172$ erg/cm^2 from the literature (*16*).

Table 1 summarizes the distances for the relaxed shapes shown in Figs. 1 and 2 and the interfacial free energy of the a-facet and s-facet. In addition, the theoretical crystal profile $z(x)$ could be calculated from the experimental values of $\beta/a \sim 0.014$ erg/cm^2 (*17*) and the step-step interaction coefficient $\sigma/a^3 \sim 1.63$ erg/cm^2 (*18*). The thick curve along the crystal surface in Fig. 4 represents $z(x)$, and the region between the open arrows in the magnified view (Fig. 4B) corresponds to the c-facet, $2R_F$. The theoretical curve was in reasonable agreement with the profile of the crystal. The inclination of the vicinal surface is shown to be so small near the facet that the border between the facet and the vicinal surface could not be macroscopically recognized. The deviation of $z(x)$ from the crystal profile occurred in the region indicated by the two-headed arrow in the magnified view of Fig. 4B, where the surface is inclined about 7° from the c-facet. The reasonable consistency between the experimental crystal profile and the theoretical curve was also confirmed for the relaxed crystal shown in Fig. 1.

In summary, the relaxation processes and subsequent relaxed shapes of ^{4}He crystals under zero gravity were strongly dependent on the initial crystal shapes and crystalline orientation. Comparison of the relaxed shape with the theoretically predicted equilibrium shape of the c-facet and the adjacent vicinal surface confirmed that the relaxed crystal achieved the equilibrium state. Although the ECS under zero gravity had macroscopically flat wide planes parallel to the c-facet, a-facet, and s-facet, the facets were only in a very narrow area around the center of the planes and the other apparently flat planes were identified as vicinal surfaces. These zero-gravity experiments have reconfirmed that the step free energies of ^{4}He crystals are much smaller than the interfacial free energies and that all facets of ^{4}He crystals can only be present on each small region under equilibrium conditions.

MATERIALS AND METHODS

A small jet plane (*19*) conducted the parabolic flight to produce a low-gravity environment for 20 s. Twenty seconds is sufficient time for the ^{4}He crystal to reach equilibrium, as long as the temperature is below 600 mK (*20*). Another experimental challenge is to develop a customized ^{3}He-^{4}He dilution refrigerator for the small jet plane. Several restrictions, such as the total weight of the equipment, available electric power, and experimental space and time, must be overcome.

A small Gifford-McMahon refrigerator (*21*) provided a 4-K stage in a vacuum chamber. Operation of the refrigerator under parabolic flight was not guaranteed because it contains a considerable amount of oil. However, the refrigerator was successfully operated many times of parabolic flights. A cylindrical container of liquid ^{4}He with a volume of 8 liters was installed inside the 4-K–stage thermal shield. The liquid container surrounded the ordinary-type dilution refrigerator unit with only a tube-in-tube heat exchanger, and it supplied the 1-K pot with the liquid. Scroll pumps were used for circulation of the ^{3}He and for the 1-K pot. The system was successfully operated down to about 140 mK onboard the aircraft. The base temperature was not affected during the 20 s of parabolic flight. The cryostat and sample cell had optical windows that enabled observation of the ^{4}He crystals. The ^{4}He crystals were illuminated from the back side, and motion pictures were acquired from the front window using a high-resolution charge-coupled device camera (*22*). The diameter of the cell windows was 24 mm, and the distance between them was 20 mm. Ultrasonic transducers were placed on the upper and lower parts of the sample cell to manipulate the crystals by acoustic radiation pressure (*23*). Thanks to the ultrahigh mobility of the crystal surface, the pressure of the system was rather uniform and stayed on the equilibrium crystallization pressure of 25 bar, although any pressure control was not made.

SUPPLEMENTARY MATERIALS

Supplementary material for this article is available at http://advances.sciencemag.org/cgi/content/full/1/9/e1500825/DC1

Movie S1. A movie of Fig. 1.

Movie S2. A movie of Fig. 2.

REFERENCES AND NOTES

1. P. Nozières, Shape and growth of crystals, in *Solids Far from Equilibrium*, C. Godrèche, Ed. (Cambridge University, Cambridge, UK, 1992).
2. S. Balibar, H. Alles, A. Ya. Parshin, The surface of helium crystals. *Rev. Mod. Phys.* **77**, 317 (2005).
3. T. Ohta, M. Fujio, K. Kawasaki, Effects of the gravitational field on the surface roughening transition. *Prog. Theor. Phys.* **61**, 74–85 (1979).
4. J. E. Avron, R. K. P. Zia, Transmutation of the vicinal surface exponent due to gravity. *Phys. Rev. B* **37**, 6611–6614 (1988).
5. M. Reivinen, E.-M. Salonen, I. Todoshchenko, V. P. Vaskelainen, Equilibrium crystal shapes by virtual work. *J. Low Temp. Phys.* **170**, 75–90 (2013).
6. T. Takahashi, R. Nomura, Y. Okuda, ^{4}He crystals in superfluid under zero gravity. *Phys. Rev. E* **85**, 030601(R) (2012).
7. P. E. Wolf, S. Balibar, F. Gallet, Experimental observation of a third roughening transition on hcp ^{4}He crystals. *Phys. Rev. Lett.* **51**, 1366 (1983).
8. R. Nomura, Y. Suzuki, S. Kimura, Y. Okuda, Interface motion and nucleation of solid helium-4 induced by acoustic waves. *Phys. Rev. Lett.* **90**, 075301 (2003).
9. R. Nomura, S. Kimura, F. Ogasawara, H. Abe, Y. Okuda, Orientation dependence of interface motion in ^{4}He crystals induced by acoustic waves. *Phys. Rev. B* **70**, 054516 (2004).
10. H. Abe, Y. Saitoh, T. Ueda, F. Ogasawara, R. Nomura, Y. Okuda, A. Ya. Parshin, Facet growth of ^{4}He crystal induced by acoustic waves. *J. Phys. Soc. Jpn.* **75**, 023601 (2006).
11. C. Jayaprakash, W. F. Saam, S. Teitel, Roughening and facet formation in crystals. *Phys. Rev. Lett.* **50**, 2017 (1983).
12. M. Uwaha, P. Nozières, Crystal shapes viewed as mechanical equilibrium of steps, in *Morphology and Growth Unit of Crystals*, I. Sunagawa, Ed. (Terra Scientific Publishing Company, Tokyo, Japan, 1989).
13. V. I. Marchenko, A. Ya. Parshin, Elastic properties of the crystal surface. *Sov. Phys. JETP* **52**, 129–131 (1980), http://www.jetp.ac.ru/cgi-bin/dn/e_052_01_0129.pdf (accessed 14 October 2015).
14. Y. Akutsu, N. Akutsu, T. Yamamoto, Universal jump of gaussian curvature at the facet edge of a crystal. *Phys. Rev. Lett.* **61**, 424–427 (1988).
15. G. Wulff, Zur frage der geschwindigkeit des wachstums und der auflösung von krystallflächen. *Z. Kristallogr.* **34**, 449–530 (1901).
16. O. A. Andreeva, K. O. Keshishev, Solid-superfluid ^{4}He interface. *Phys. Scr.* **T39**, 352 (1991).
17. E. Rolley, C. Guthmann, E. Chevalier, S. Balibar, The static and dynamic properties of vicinal surfaces on helium 4 crystals. *J. Low Temp. Phys.* **99**, 851–886 (1995).

18. K. O. Keshishev, D. B. Shemyatikhin, Contact angle singularity in ^{4}He crystals. *J. Low Temp. Phys.* **150**, 282–288 (2008).
19. Diamond Air Service Inc., 1 Toyoba, Toyoyama-cho, Nishikasugai-gun, Aichi 489-0293, Japan.
20. T. Takahashi, M. Suzuki, R. Nomura, Y. Okuda, Development of a ^{3}He refrigerator for possible experiments of solid ^{4}He on a small jet plane. *J. Low Temp. Phys.* **162**, 733–739 (2011).
21. Sumitomo Heavy Industries Ltd., Model RDK-101D.
22. Keyence Corporation, Model VH500, www.keyence.com/www.keyence.com/.
23. Y. Okuda, R. Nomura, New aspects of crystal growth of solid ^{4}He studied by acoustic wave. *J. Phys. Soc. Jpn.* **77**, 111009 (2008).

Funding: This study was supported in part by the Nanoscience and Quantum Physics Project of the Tokyo Institute of Technology Global Center of Excellence, a Grant-in-Aid for Scientific Research (nos. 21340095 and 26287074) from the Ministry of Education, Culture, Sports, Science and Technology of Japan, and by the Ground-based Research Announcement for Space Utilization promoted by the Japan Aerospace Exploration Agency. T.T. acknowledges the support of a Research Fellowship of the Japan Society for the Promotion of Science for Young Scientists (grant no. 24·8723). H.O. acknowledges the support of the Academy for Global Leadership. **Author contributions:** Y.O. and R.N. planed and supervised the project. T.T. and H.O. conducted the experiment and analyzed the data. T.T., Y.O., and R.N. wrote the manuscript. All authors discussed the results. **Competing interests:** The authors declare that they have no competing interests. **Data and materials availability:** All relevant data to support the conclusions are within the paper and its Supplementary Materials. The authors will make raw data available upon request at nomura.r.aa@m.titech.ac.jp.

Submitted 22 June 2015
Accepted 17 July 2015
Published 23 October 2015
10.1126/sciadv.1500825

Citation: T. Takahashi, H. Ohuchi, R. Nomura, Y. Okuda, Equilibrium shape of ^{4}He crystal under zero gravity below 200 mK. *Sci. Adv.* **1**, e1500825 (2015).

Science Advances

Equilibrium shape of ^{4}He crystal under zero gravity below 200 mK

Takuya Takahashi, Haruka Ohuchi, Ryuji Nomura and Yuichi Okuda

Sci Adv **1** (9), e1500825.
DOI: 10.1126/sciadv.1500825